

# Thermal and Mechanical Properties of Polystyrene/Poly(acrylonitrile-g-(ethylene-co-propylene-co-diene)-g-styrene) (AES) Blends Prepared by the *In Situ* Polymerization of Styrene

Emerson Lourenço, Maria Isabel Felisberti

Instituto de Química, Universidade Estadual de Campinas, Caixa Postal 6154, 13084-862 Campinas, SP, Brazil

Received 6 November 2006; accepted 1 February 2007

DOI 10.1002/app.26330

Published online 6 April 2007 in Wiley InterScience (www.interscience.wiley.com).

**ABSTRACT:** Polystyrene/AES blends formed by the *in situ* polymerization of styrene in the presence of poly(acrylonitrile-g-(ethylene-co-propylene-co-diene)-g-styrene) (AES) were prepared. AES is a commercial elastomer obtained by the radical copolymerization of styrene and acrylonitrile in the presence of an ethylene-propylene-diene terpolymer (EPDM). The polystyrene/AES blends presented two phases: an EPDM elastomeric phase dispersed in a rigid matrix. The phase behavior was strongly affected by the polymerization temperature. The blends showed higher thermal stability than the polystyrene homopolymer because of the stabilizing effect of EPDM incorporation. The

mechanical properties were influenced by the polymerization temperature and blend composition. The blend prepared at 60°C with 13.0 wt % AES presented an enhancement of 60% in the impact resistance, whereas the blend prepared at 80°C with 21.8 wt % AES presented an enhancement of 150% in the strain at break. Both blends had these properties improved with a small loss in the Young's modulus. © 2007 Wiley Periodicals, Inc. *J Appl Polym Sci* 105: 986–996, 2007

**Key words:** blends; mechanical properties; radical polymerization; thermal properties

## INTRODUCTION

Polymer blending is a simple and efficient method for designing and controlling the thermal and mechanical properties of polymeric materials using easily available polymers.<sup>1</sup> Most polymer pairs in blends are thermodynamically immiscible and also incompatible. Incompatible blends often do not show improvements in the mechanical properties because of poor interfacial adhesion and the lack of physical and chemical interactions between different phases.<sup>2,3</sup> The incorporation of dispersed elastomeric particles into a rigid polymer matrix has attracted considerable attention because of its industrial importance among other types of polymer blends.<sup>4–6</sup> Cavanaugh et al.<sup>7</sup> observed an enhancement of 800% in the impact resistance of polystyrene (PS)/polybutadiene blends (23 vol % rubber) compatibilized with a PS-polybutadiene block copolymer in comparison with PS. This enhancement was attributed to the long asymmetric chain of the diblock compatibilizer, which was capable of entangling in both homopolymer phases. Neoh

and Hashim<sup>8</sup> prepared PS/natural rubber and PS/polystyrene-g-natural rubber blends by mechanical mixing and obtained enhancements of 180 and 350% in the impact resistance, respectively, in comparison with PS.

One way of improving the compatibility among different polymers is the *in situ* polymerization of the monomer in the presence of the rubber phase, as in the production of high-impact polystyrene (HIPS).<sup>9–11</sup> Sardelis et al.<sup>12</sup> produced poly(styrene-b-butadiene-b-styrene) (SBS) toughened PS by the *in situ* polymerization of styrene in the presence of 6.5 wt % SBS with a molar mass of 22,000 g/mol and observed a three-fold increase in the impact resistance in comparison with PS.

Acrylonitrile-butadiene-styrene (ABS) and HIPS are good examples in which the mechanical properties can be modified through a change in the microstructure of the rubbery particles. The rubbery chains are grafted into the rigid polymeric matrix, and this grafting enhances the interfacial bonding between the phases, providing a good dispersion of the elastomeric particles in the polymeric matrix matching the thermodynamic parameters.<sup>13</sup> Besides its direct technological application, HIPS is also used in blends with other polymers,<sup>4,14</sup> such as poly(2,6-dimethyl-1,4-phenylene oxide), which is widely applied in the automotive industry and in home appliances.<sup>9,15</sup> Aging is a great problem for HIPS and other rubber-

Correspondence to: M. I. Felisberti (misabel@iqm.unicamp.br).

Contract grant sponsor: Fundação de Amparo à Pesquisa do Estado de São Paulo; contract grant number: 03/04246-2.

toughened plastics, especially those based on polybutadiene. Exposure to sunlight causes a drastic drop in the impact resistance that is attributed to the photooxidation of the rubber phase induced by UV radiation, limiting the lifetime of molded parts in outdoor applications.<sup>9,10,16</sup> To overcome this problem, the replacement of polybutadiene by a saturated rubber such as ethylene/vinyl acetate (EVA), butyl acrylate, chlorinated polyethylene, or ethylene-propylene-diene terpolymer (EPDM) has been suggested.<sup>11,17,18</sup> Cheng et al.<sup>19</sup> prepared EVA-toughened PS by the *in situ* polymerization of styrene, using benzoyl peroxide as an initiator and *tert*-butyl peroxoate for chain transfer. The addition of 10 wt % EVA to PS increased the impact resistance and strain at break of PS by a factor of 5 but reduced the modulus by the same factor for blends containing high-molar-mass EVA. Shaw and Singh<sup>20–22</sup> used graft copolymers of EPDM with PS (EPDM-*g*-PS), poly(styrene-*co*-methyl methacrylate) [EPDM-*g*-(PS-*co*-MMA)], and poly(styrene-*co*-maleic anhydride) [EPDM-*g*-(PS-*co*-MAH)] to prepare blends with PS by mechanical mixing. They obtained blends with an enhancement of the impact resistance of 400% for a PS/EPDM-*g*-(PS-*co*-MMA) (96/4) blend and for a PS/EPDM-*g*-(PS-*co*-MAH) (94/6) blend and of 500% for a PS/EPDM-*g*-PS (90/10) blend. They attributed these improvements in the impact resistance to the compatibilization of the graft copolymers of EPDM with the PS matrix resulting from good interfacial adhesion.

ABS is another important commercial polymer that presents high impact resistance, stiffness, easy production, and processability that justify its application in the automotive industry. However, ABS presents low thermal resistance and low weatherability because of the high level of unsaturation of its rubber phase. In this way, research in this field has led to the production of a thermoplastic with a low level of unsaturation, the polymer poly(acrylonitrile-*g*-(ethylene-*co*-propylene-*co*-diene)-*g*-styrene) (AES). AES is very attractive because of its appreciable impact resistance and better environmental and thermal resistance versus ABS and polybutadiene due to the low amount of unsaturation of EPDM rubber.<sup>16</sup> AES is a commercial elastomer obtained by the radical copolymerization of styrene and acrylonitrile in the presence of EPDM. Poly(styrene-*co*-acrylonitrile) (SAN) is formed, either grafted onto EPDM chains or ungrafted. The final product also contains a fraction of EPDM molecules not involved in the grafting process.<sup>23</sup>

Turchet<sup>23</sup> prepared poly(methyl methacrylate) (PMMA)/AES blends by mechanical mixing and obtained a toughened blend with 30 wt % AES. This blend exhibited an increase of 990% in the impact resistance, in comparison with PMMA, because of an SAN compatibilizing effect, improving the adhesion and dispersion of EPDM particles in the PMMA ma-

trix. Lu et al.<sup>24</sup> evaluated the mechanical properties of nylon 6/ABS (55/45) and nylon 6/AES (55/45) blends prepared by mechanical mixing. They observed for both blends the same decrease in the strain at break of 83% in comparison with the value for nylon 6 and attributed the decrease to the low adhesion between the phases and a morphology that presented large ABS and AES domains. However, they also observed higher enhancements of the impact resistance of 80 and 60% for nylon 6/AES and nylon 6/ABS blends, respectively, in comparison with nylon 6 values. Larocca et al.<sup>16</sup> obtained a super-tough poly(butylene terephthalate) (PBT)/AES blend. An increase of 1600% in the impact resistance of a blend containing 30 wt % AES was observed. AES particles may be able to relieve the high triaxial stress at the notch tip, allowing local shear yielding of the PBT matrix and therefore promoting high mechanical energy absorption by the system.

In this context, the aim of this work is to prepare and evaluate the thermal and mechanical properties of *in situ* polymerized PS/AES blends that exhibit higher thermal stability and photostability than PS and HIPS.<sup>25</sup>

## EXPERIMENTAL

### Materials

Rhodia Brazil (Paulina, Brazil) supplied styrene. Crompton Corp. (Rio Claro, Brazil) supplied AES (Royaltuf 372P20). AES is a complex mixture of SAN, EPDM, and the graft copolymer EPDM-*g*-SAN. AES contains 13 wt % free EPDM, 22 wt % free SAN, and approximately 65 wt % EPDM-*g*-SAN. SAN presents 27 wt % acrylonitrile. The global composition of AES is 50 wt % SAN and 50 wt % EPDM. EPDM of AES contains 68.9 wt % ethylene, 26.5 wt % propylene, and 4.6 wt % 2-ethylidene-5-norbornene as a diene.<sup>23</sup>

### Styrene monomer purification

Styrene monomer was subjected to the extraction of polymerization inhibitors with a 5% NaOH solution. After this, the organic layer was washed with distilled water. The water residue was extracted with dry Na<sub>2</sub>SO<sub>4</sub>, and the styrene was then distilled at 50°C *in vacuo*.

### PS/AES blends prepared by the *in situ* polymerization of styrene

AES was dissolved in styrene monomer under stirring, then benzoyl peroxide (0.1 wt %) was added to the viscous and homogeneous solution, and the polymerization was carried out at 60 or 80°C for 168 h. After this, the styrene monomer residue (~ 5 wt %) was extracted at 50°C in a vacuum oven for 48 h. The PS

homopolymer was also prepared at 60 and 80°C. The polymerization reactions yielded a 92% conversion.

### Elemental analysis

The AES content in the PS/AES blends was calculated from the nitrogen percentage of the blends, which was obtained with a PerkinElmer (Waltham, MA) 2400 elemental analyzer.

### Gel permeation chromatography

The homopolymer PS was extracted from the blends with dichloromethane for 72 h with a Soxhlet apparatus. The extracted PS corresponded to 80 wt % of the synthesized PS. The weight-average molar weight ( $M_w$ ), number-average molar weight ( $M_n$ ), and polydispersity ( $M_w/M_n$ ) of the PS matrix were measured by gel permeation chromatography in a Waters (Milford, MA) 510 gel permeation chromatograph with a Waters 410 differential refractometer detector. Separation was performed on PS-divinylbenzene Tosoh-Haas (Montgomeryville, PA) columns with 10- $\mu$ m particles. High performance liquid chromatograph (HPLC)-grade tetrahydrofuran was used as mobile phase at a flow rate of 1 mL/min.

### Tensile and impact resistance tests

The crushed PS/AES blends were dried in a vacuum oven for 48 h at 50°C and injection-molded into Izod bars (ASTM D 256) and dog-bone-shaped tensile specimens (ASTM D 638) with an Arburg Allrounder (Lassburg, Germany) model 221 M 250-55 molding machine. The following temperatures were kept along the barrel zones: 200, 210, 220, 230, and 240°C. The mold temperature was kept at 40°C. The injection-molded specimens were submitted to impact resist-

ance and tensile tests in an Emic (São José dos Pinhais, Brazil) AIC 1 apparatus and in an Emic DL 200 apparatus (5000 N load cell, 5 mm/min speed), respectively.

### Dynamic mechanical analysis (DMA)

Blend specimens (9.0 mm  $\times$  6.0 mm  $\times$  1.0 mm) were subjected to sinusoidal deformation at a frequency of 1.0 Hz and amplitude of 0.01% in the temperature range from -100 to 180°C in a Rheometric Scientific (Piscataway, NJ) DMTA V analyzer.

### Thermogravimetric analysis (TGA)

TGA of the injection-molded specimens was performed with a TA Instruments (New Castle, DE) 2950 thermogravimetric analyzer in the temperature range of 40–600°C at a heating rate of 10°C/min under air or argon flows (100 dm<sup>3</sup>/min).

### Scanning electron microscopy (SEM)

The fracture surfaces obtained during Izod impact resistance tests were covered by a carbon layer produced by direct sputtering and observed with a JEOL (Middleton, WI) JSM-6360 LV scanning electron microscope at an acceleration voltage of 20 kV.

## RESULTS AND DISCUSSION

In this work, *in situ* polymerized PS/AES blends were prepared at 60°C and at 80°C with the aim of obtaining rubber-toughened PS and of analyzing the influence of different polymerization temperatures on the thermal and mechanical properties of these blends.

TABLE I  
PS/AES Blends Prepared in This Work

Name	AES in a styrene solution (wt %) <sup>a</sup>	AES in a blend (wt %) <sup>b</sup>	EPDM in a blend (wt %) <sup>c</sup>	$M_w$ of PS ( $\times 10^3$ g/mol)	$M_n$ of PS ( $\times 10^3$ g/mol)	$M_w/M_n$	Reaction temperature (°C)
3.7A60	4	7.3	3.7	455	271	1.7	60
4.5A60	7	9.0	4.5	463	265	1.7	60
6.5A60	10	13.0	6.5	585	283	2.1	60
7.9A60	13	15.8	7.9	628	268	2.3	60
9.5A60	16	18.9	9.5	678	298	2.3	60
11.5A60	19	22.9	11.5	669	316	2.1	60
7.2A80	10	14.4	7.2	228	98	2.3	80
8.5A80	13	17.0	8.5	541	188	2.9	80
9.4A80	16	18.8	9.4	392	187	2.1	80
10.9A80	19	21.8	10.9	373	173	2.2	80
PS60	—	—	—	367	140	2.6	60
PS80	—	—	—	419	193	2.2	80

<sup>a</sup> AES content dissolved in a styrene solution.

<sup>b</sup> AES content obtained from elemental analysis.

<sup>c</sup> EPDM content obtained from the AES content in a blend.

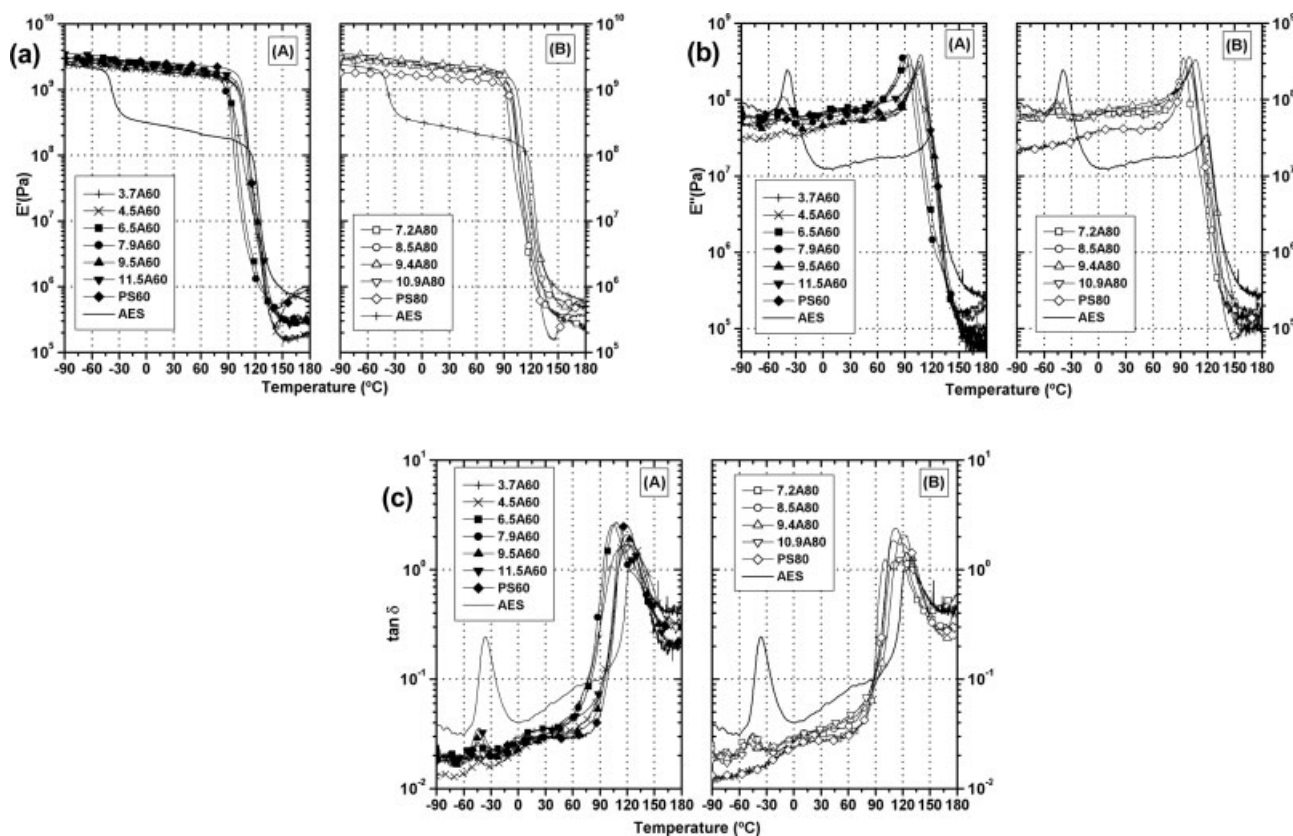


**Figure 1** Dynamic mechanical behavior of PS60, PS80, AES, and PS/AES blends: (a)  $E'$ , (b)  $E''$ , and (c)  $\tan \delta$  curves. The blends were prepared at (A) 60 and (B) 80°C.

The AES/styrene solution is transparent, and this indicates that the solution is homogeneous; when styrene polymerizes, the solution becomes opaque because PS is immiscible with SAN and EPDM.

The styrene polymerization yielded at least a 92% conversion for all compositions and temperatures of polymerization, as determined gravimetrically, presenting the tendency of a slight increase as the temperature increased.

Table I shows the compositions of the AES solutions in styrene, the compositions of the PS/AES blends expressed in terms of the weight percentage of AES in the blends, and the EPDM contents in each blend. The AES content in the blends was calculated from the nitrogen percentage determined by elemental analysis. The nomenclature used to describe the blends is based on the EPDM content and on the temperature of polymerization. For example, the blend containing 11.5 wt % EPDM polymerized at 60°C is named 11.5A60, where A represents the source of EPDM, AES.

The polydispersity of the extracted PS from the blends is between 1.7 and 2.9, being independent of the blend composition and temperature of polymerization. The average molar mass of the PS/AES blends is between 228,000 and 678,000 g/mol and

shows a tendency to increase with the increase in the AES content for blends obtained at 60°C, whereas it does not show a coherent behavior for the blends polymerized at 80°C.

**TABLE II**  
Glass-Transition Temperatures of EPDM and PS/SAN-Rich Phases Obtained from  $E''$  Curves and  $\tan \delta$  Curves for Injection-Molded PS/AES Blends

Material	Glass-transition temperature (°C)			
	EPDM phase		PS/SAN-rich phase	
	$E''$	$\tan \delta$	$E''$	$\tan \delta$
3.7A60	—	—	96	116
4.5A60	-48	-44	106	119
6.5A60	-45	-45	94	107/121
7.9A60	-47	-45	91	105/132
9.5A60	-44	-42	106	114/124
11.5A60	-44	-43	106	114/124
7.2A80	-48	—	94	100/120
8.5A80	-46	-48	100	112
9.4A80	-46	-46	107	122
10.9A80	-40	-45	102	111/124
PS60	—	—	108	119
PS80	—	—	101	109
AES	-40	-37	119	128

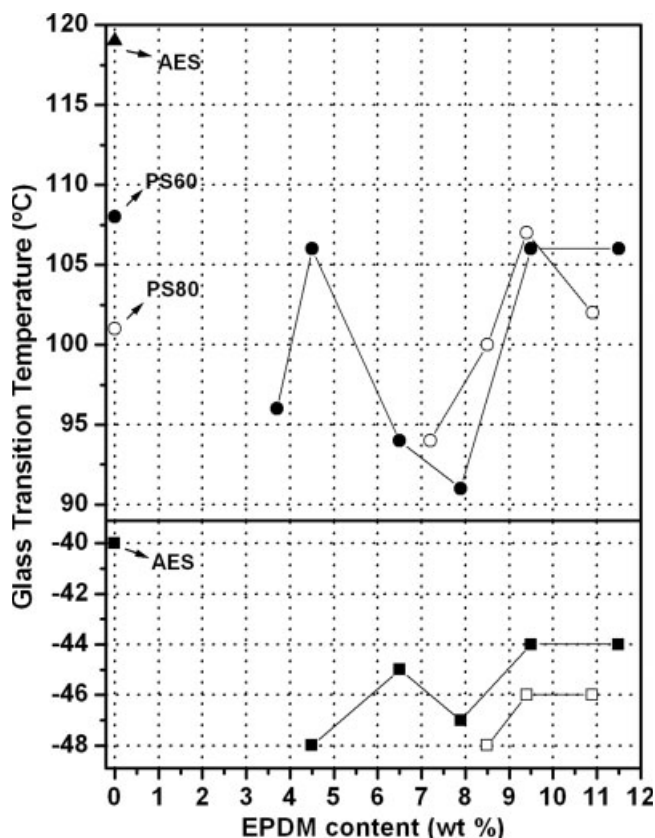


**Figure 2** Glass-transition temperature as a function of the EPDM content for injection-molded PS60, PS80, AES, and PS/AES blends prepared at 60°C (solid symbols) and 80°C (open symbols): (■,□) EPDM, (●,○) PS, and (▲) SAN phases.

## DMA

Figure 1 shows the dynamic mechanical behavior of PS60, PS80, AES, and PS/AES blends. The glass-transition temperatures were obtained from the maximum of the loss modulus ( $E''$ ) peaks in the  $E''$ /temperature curves and of the damping ( $\tan \delta$ ) peaks in the  $\tan \delta$ /temperature curves. The values are shown in Table II. The storage modulus ( $E'$ ) curves for PS60 and PS80 [Fig. 1(a)] show a drastic drop around 95°C corresponding to the glass transition of PS. The AES curve shows a drop of a decade around -40°C corresponding to the glass transition of the EPDM phase and another drop of 2 decades at 119°C corresponding to the SAN glass transition.<sup>16</sup> The  $E'$  values of all PS/AES blends show little change at the EPDM glass-transition region ( $\sim -40^\circ\text{C}$ ) and a drop of 3 decades in the region of the PS/SAN glass transition ( $\sim 120^\circ\text{C}$ ). This behavior indicates that the morphology of the PS/AES blends is of dispersed elastomeric domains (EPDM) in the glassy matrix (PS/SAN). The  $\tan \delta$  curves for the PS/AES blends [Fig. 1(c)] show a small peak at approximately 60°C that is attributable

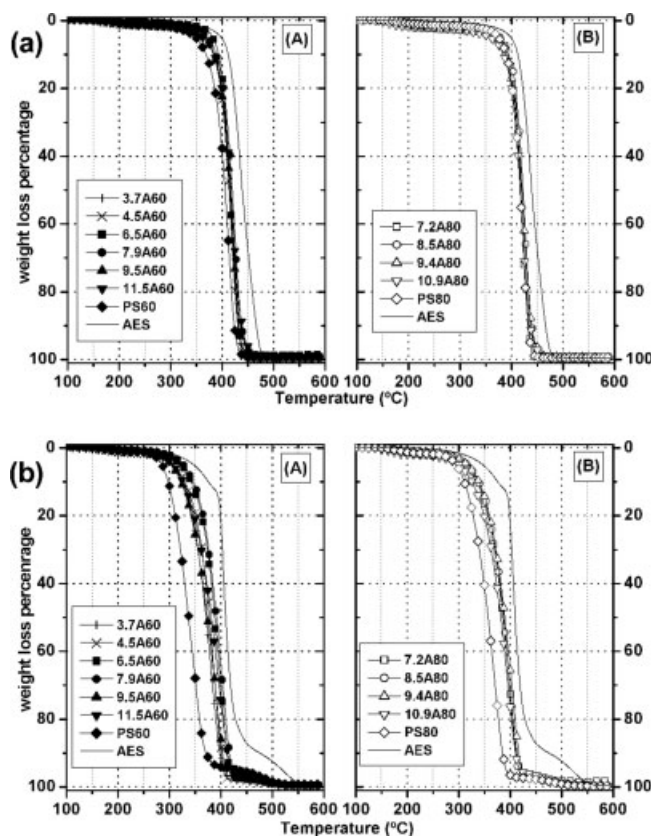
to a secondary transition of the EPDM phase. Sheng et al.<sup>26</sup> also observed a liquid–liquid transition for EPDM by thermally stimulated current at approximately 100°C. Keinath and Boyer<sup>27</sup> described the liquid–liquid transition as a relaxation above the glass-transition temperature at which the material experiences increased fluidity.

Figure 2 shows the glass-transition regions of PS and SAN. The glass transition of SAN is higher than those of PS60 and PS80. The rigid phase of the blends presents a complex phase behavior, and their  $E''$  curves present peaks and shoulders associated with different phases. The peak at a lower temperature is presumed to be related to the glass transition of the PS phase, and the other peak at a higher temperature is related to the SAN phase. The temperature range in which these peaks appear is a function of the blend composition and polymerization temperature, as can be clearly seen in Figure 2. Hachiya et al.<sup>28,29</sup> indicated that PS is partly miscible with SAN containing less than 5 wt % acrylonitrile. Fekete et al.<sup>30</sup> also observed from tensile strength tests, differential scanning calorimetry, and the Flory–Huggins interaction parameter derived from the Hildebrand solubility parameter that PS and SAN blends are thermodynamically immiscible and incompatible.

The EPDM phase of all blends presents a glass-transition temperature at a lower temperature than the EPDM phase of AES (Table II and Fig. 2). This behavior was also observed in an earlier work of our research group with PMMA/AES blends.<sup>23</sup> This shift to lower temperatures is attributed to the phase inversion of the EPDM phase of AES during AES dissolution in styrene monomer and its *in situ* polymerization. EPDM is the matrix in AES, whereas SAN and EPDM-g-SAN chains constitute the dispersed phase. In the blends, EPDM becomes the dispersed phase, and the release of the SAN chains from the elastomeric phase can contribute to the decrease in the EPDM glass-transition temperature.<sup>23</sup> This behavior in blends of a rubbery phase dispersed in glassy matrices is common and is attributed to hydrostatic dilatational thermal stresses generated within the rubber particles because of the differences in the thermal expansion between the rubber and the glassy matrix. This dilatational stress promotes an increase in the rubbery phase free volume, which allows the reduction of the relaxation time of the rubbery chains and therefore reduces the glass-transition temperature of the corresponding phase.<sup>16,31</sup>

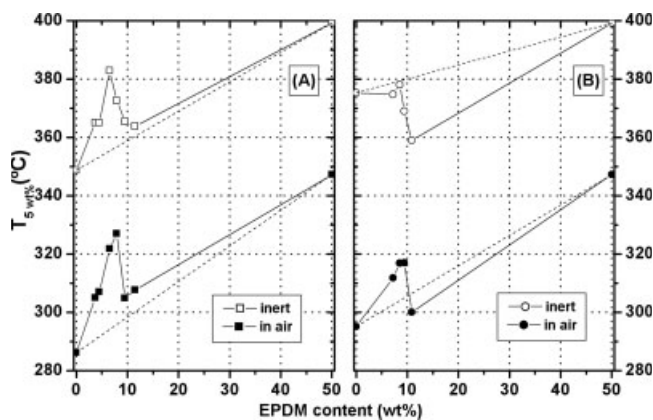
## TGA

Figure 3 presents thermogravimetric curves for PS60, PS80, AES, and PS/AES blends in air and under an inert atmosphere. PS80 shows higher thermal and thermooxidative stability than PS60.



**Figure 3** Thermogravimetric curves (a) under an inert atmosphere and (b) in air for PS60, PS80, AES, and PS/AES blends. The blends were prepared at (A) 60 and (B) 80°C.

AES is more stable than neat PS in both oxidative and inert atmospheres. Under an inert atmosphere, AES presents only one weight-loss process and presents several processes in air beginning at lower temperatures. The decomposition of AES can be understood as a sum of EPDM and SAN degradations.<sup>32</sup> SAN decomposes by depolymerization, leading to the formation of low-molar-mass products. Radicals from SAN degradation abstract hydrogen from EPDM, yielding EPDM macroradicals.<sup>23</sup> At the beginning of degradation, EPDM chains react with oxygen, yielding hydroperoxides that decompose into hydroxyl and carbonyl groups. This reaction occurs by a typical mechanism of hydrocarbon oxidation, involving secondary and tertiary carbon atoms on the propylene units. The high reactivity of EPDM in the EPDM-g-SAN copolymer is associated with the presence of the SAN chains attached to the diene. Because the formation of the tertiary radical occurs at the carbon to which the SAN chain is attached, this radical accelerates the reaction with oxygen. The decomposition of the peroxide and the addition to the double bond leads to the stiffening of AES, whereas chain scission results in a molar mass decrease.<sup>33</sup>



**Figure 4** Temperature of 5 wt % mass loss ( $T_{5wt\%}$ ) as a function of the EPDM content for PS60, PS80, AES, and PS/AES blends. The blends were prepared at (A) 60 and (B) 80°C.

The blends and neat PS show a small weight-loss process ( $\sim 2\text{--}3\%$ ) at approximately 180°C probably due to the presence of volatile oligomers. Under the inert atmosphere, the significant weight-loss process begins at approximately 350°C, whereas it begins at approximately 300°C in air. The blends prepared at 60°C show higher thermal and thermooxidative stability than neat PS because of the stabilization of AES caused by EPDM, deactivating PS macroradicals through intermolecular reactions with structural units of EPDM.<sup>34</sup> This stabilization is also observed in Figure 4, in which the temperature of a 5 wt % loss is plotted as a function of the AES content. A positive deviation from the additive rule (dashed lines) is observed for all blends prepared at 60°C, indicating that the addition of AES into a PS matrix stabilizes the blends. A negative deviation from the additive rule is observed for almost all blends prepared at 80°C. These differences of the thermal and thermooxi-

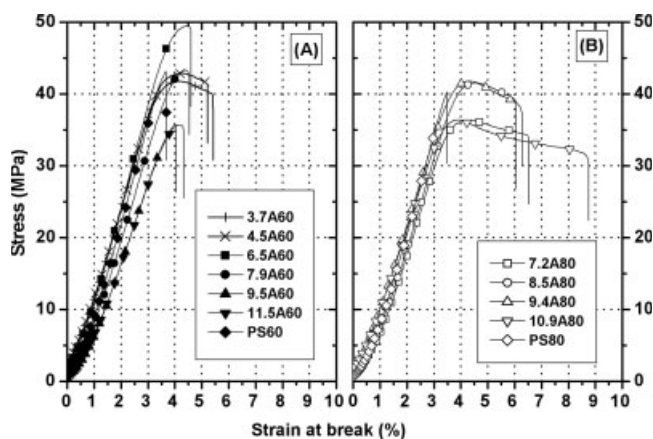


**Figure 5** Representative stress-strain curves for PS60, PS80, and PS/AES blends. The blends were prepared at (A) 60 and (B) 80°C.

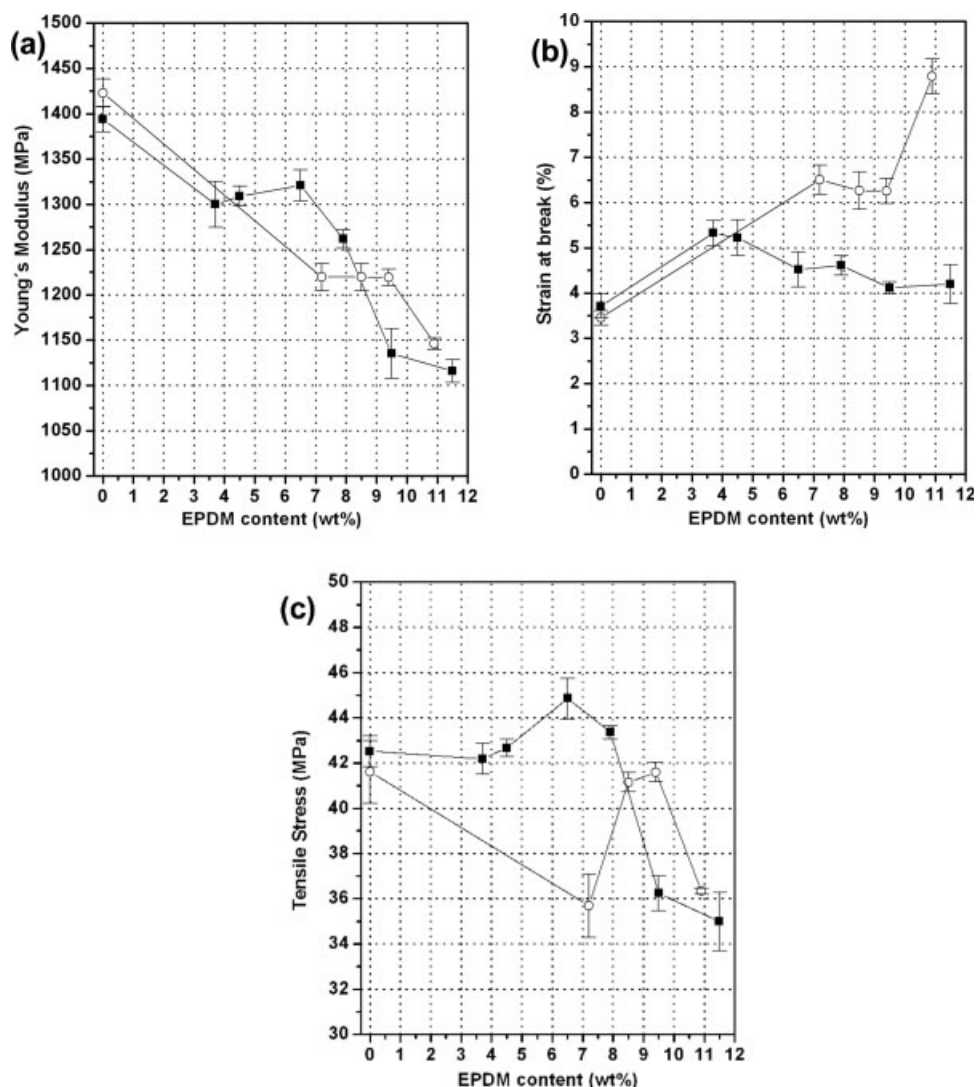


**Figure 6** (a) Young's modulus, (b) strain at break, (c) and tensile stress curves as a function of the EPDM content for PS/AES blends prepared at (■) 60 and (○) 80°C.

dative behavior between the blends prepared at 60 and 80°C suggest that blends with similar global compositions do not present the same constituents. During the styrene polymerization, other reactions can take place, such as the grafting of styrene onto SAN and EPDM chains, besides crosslinking reactions, as observed by the formation of an insoluble gel phase extracted from the PS/AES blends prepared in this work (2–25 wt %). The relative concentration of these species could affect the thermal and thermooxidative processes.

#### Tensile test (ASTM D 638)

Figure 5 shows representative stress–strain curves obtained from tensile tests for PS60, PS80, and PS/AES blends. The mechanical properties, such as the Young's modulus and strain at break, obtained from these curves are shown in Figure 6. The PS/AES

blends showed stress whitening during the tensile tests, indicating that dilatational processes, such as crazing and cavitation, occur during the loading.<sup>16</sup>

The Young's modulus of PS60 decreases about 7% with the addition of 3.7 wt % EPDM (7.3 wt % AES), remains constant up to 6.5 wt % EPDM (13.0 wt % AES), and then drops 20% in comparison with the value of PS. For the blends obtained at 80°C, the Young's modulus drop is more accentuated at lower elastomer contents and reaches values similar to those of the blends of comparable compositions polymerized at 60°C. These results suggest the influence of the polymerization temperature on the extent of phase segregation of the blend constituents and on the morphology. The decrease in the modulus with increasing elastomer content is expected and well reported for the rubber toughening of rigid polymers.<sup>11</sup> However, the decrease in the Young's modulus of PS/AES is lower in comparison with PS/EPDM

blends with comparable contents of the elastomer obtained by *in situ* polymerization<sup>35</sup> because of the stiffening of PS promoted by the SAN phase and also the increase in the immiscibility of PS and SAN.<sup>30</sup> In our research group, Turchet<sup>23</sup> prepared PMMA/AES blends by mechanical mixing and obtained a toughened blend with 30 wt % AES. This blend exhibited an increase of 990% in the impact resistance and only a slight decrease in the Young's modulus of 7% in comparison with the values of neat PMMA. The first result is due to the compatibilizing effect of SAN improving the adhesion and dispersion of EPDM particles in the PMMA matrix, and the second can be attributed to the stiffness of the SAN phase. Cheng et al.<sup>19</sup> prepared EVA-toughened PS by *in situ* polymerization, using benzoyl peroxide as an initiator and *tert*-butyl peroxoate as a chain-transfer reagent. The addition of 10 wt % EVA decreased the Young's modulus by a factor of 5 with a high-molar-mass EVA with 18 wt % vinyl acetate. In this work, the addition of 11.5 wt % EPDM caused a drop of the Young's modulus of about 30%, which was independent of the polymerization temperature.

In general, PS/AES blends polymerized at 80°C present a higher strain at break than blends obtained at 60°C. For the blends prepared at 60°C, the strain at break varies from 4.2 to 6.3% versus 3.4% for PS60. The PS/AES blend prepared at 80°C containing 10.9 wt % EPDM (21.8 wt % AES) presents a higher strain at break, 8.8%, versus 6.3% for the blend with a similar composition obtained at 60°C.

Larocca et al.<sup>16</sup> observed a decrease in the strain at break with increasing AES content in PBT/AES blends and attributed this effect to the premature fracture in PBT/AES blends prepared by mechanical mixing caused by the formation of macroscopic voids in the necked region of the tensile specimens, which grow readily under high stress, leading to fracture of the material. The source of such voids was attributed to several possible dilatational processes in these blends, such as a cavitation process of the rubbery phase of AES (EPDM), crazes in the SAN phase of AES, and debonding at the PBT–AES interface.<sup>16</sup> Lu et al.<sup>24</sup> evaluated the mechanical properties of nylon 6/ABS (55/45) and nylon 6/AES (55/45) blends prepared by mechanical mixing. They observed for both blends the same decrease of 83% in the strain at break in comparison with the value of nylon and attributed this decrease to low adhesion between the phases and the morphology that presents large ABS and AES domains. Bassani et al.<sup>36</sup> also studied nylon 6/AES blends, using poly(methyl methacrylate–maleic anhydride) (PMMA–MA, 1.3 wt % MA), and obtained an enhancement of the strain at break of 73% in comparison with the nylon 6 value for a nylon 6/AES/PMMA–MA (66.5/28.5/5) blend. The compatibilization with PMMA–MA led to good AES dispersion

into the matrix and better adhesion between the phases. Sardelis et al.<sup>12</sup> produced SBS-toughened PS by *in situ* polymerization with 6.5 wt % SBS with a molar mass of 22,000 g/mol, increasing the strain at break to 10%. Turchet<sup>37</sup> found for a PS/AES blend containing 50 wt % AES and prepared by mechanical mixing a strain at break of 7.5% and a Young's modulus of 629 MPa. In this work, a strain at break of  $8.8 \pm 0.4\%$  and a Young's modulus of  $1228 \pm 18$  MPa were obtained for the *in situ* polymerization of a PS/AES blend containing 10.9 wt % EPDM (21.8 wt % AES).

For blends prepared at 60°C, an increase in the AES content leads to a slight increase in the tensile stress [Fig. 6(c)] from  $42.5 \pm 0.7$  MPa for PS60 to  $44.9 \pm 0.9$  MPa for the blend containing 6.5 wt % EPDM (13.0 wt % AES). This increase in the tensile stress may be attributed to the stiffening of PS by the SAN phase. For higher AES contents, the increase in the AES content leads to a decrease in the tensile stress. For the blends prepared at 80°C, the tensile stress is lower than that of PS80, except for the blend containing 9.4 wt % EPDM (18.8 wt % AES), whose tensile stress is comparable to the value of PS80.

#### Izod impact resistance test (ASTM D 256)

The polymerization temperature also influences the Izod impact resistance (Fig. 7); the values are higher for blends prepared at 60°C than for those prepared

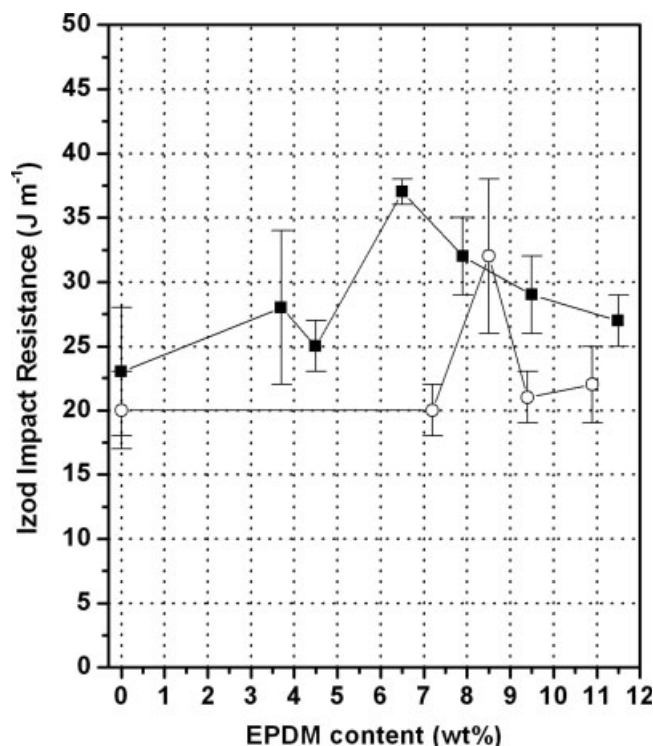


**Figure 7** Izod impact resistance as a function of the EPDM content for PS/AES blends prepared at (■) 60 and (○) 80°C.



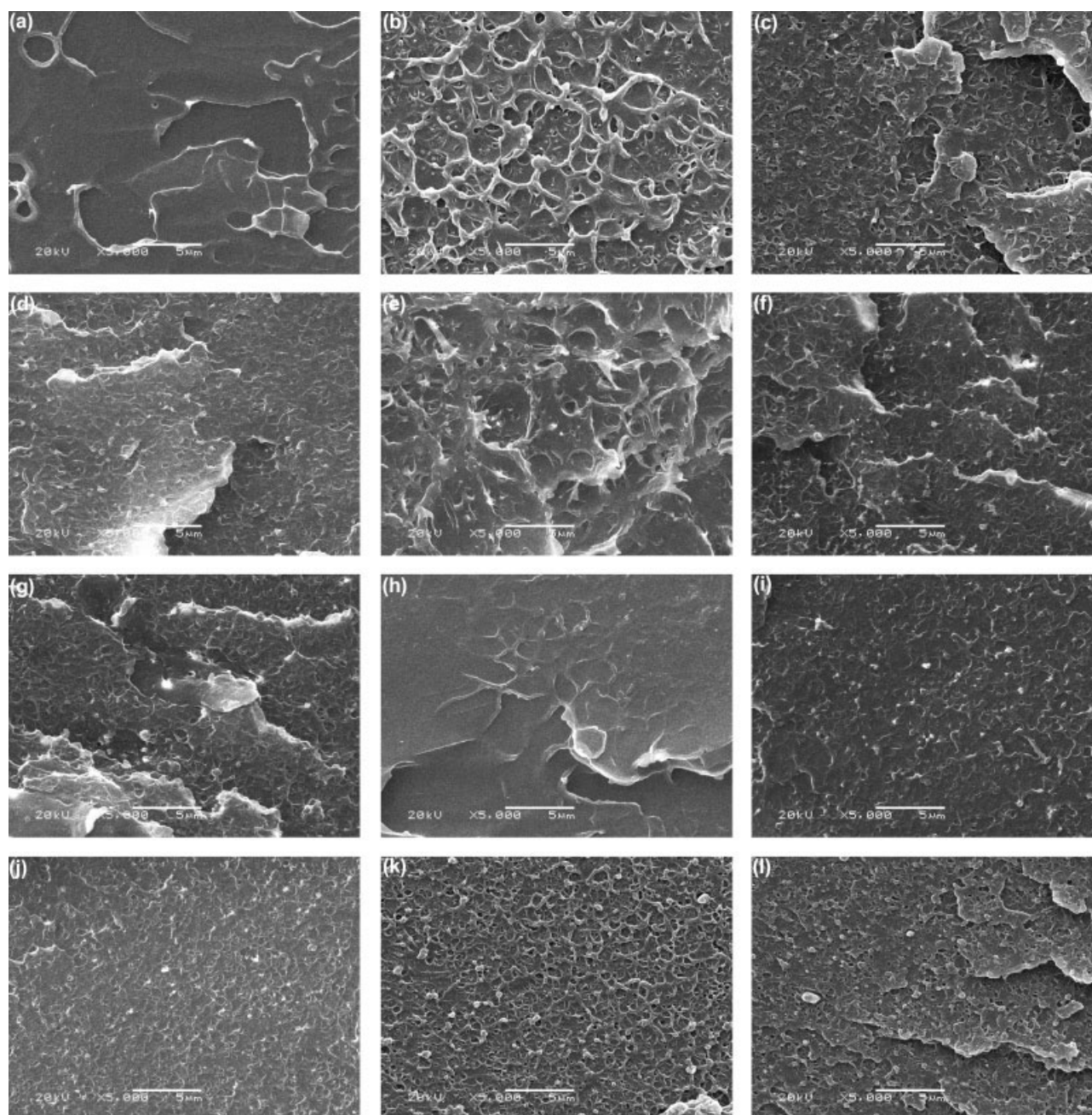


**Figure 8** SEM photographs of fracture surfaces resulting from Izod impact resistance tests: (a) PS60, (b) 3.7A60, (c) 4.5A60, (d) 6.5A60, (e) 7.9A60, (f) 9.5A60, (g) 11.5A60, (h) PS80, (i) 7.2A80, (j) 8.5A80, (k) 9.4A80, and (l) 10.9A80.

at 80°C. For the blends prepared at 60°C, an increase in the AES content up to 13.0 wt % AES (6.5 wt % EPDM) leads to an increase from  $23 \pm 5$  J/m for PS60 to  $37 \pm 1$  J/m, an enhancement of 60%, and the subsequent increase in the AES content leads to a slight decrease in the impact resistance. For the blends prepared at 80°C, the impact resistance is practically constant and equal to the value of PS80, except for the blend containing 8.5 wt % EPDM (17.0 wt % AES), whose impact resistance is  $32 \pm 6$  J/m. Larocca et al.<sup>16</sup> observed an increase of 260% in the impact resistance of a PBT/AES blend containing 20 wt % AES

compared with neat PBT. In our research group, a PS/AES blend with 50 wt % AES prepared by mechanical mixing exhibited an impact resistance of 44 J/m and a Young's modulus of 629 MPa.<sup>37</sup> An impact resistance of  $37 \pm 1$  J/m and a Young's modulus of  $1321 \pm 17$  MPa were obtained for *in situ* polymerized PS/AES blends with 13.0 wt % AES. PMMA/AES blends with 20 wt % AES prepared by mechanical mixing presented an enhancement of 36% in the impact resistance and a slight decrease in the Young's modulus of 7% in comparison with the PMMA value because of the SAN stiffening effect.<sup>23</sup>

TABLE III  
Izod Impact Resistance and Strain at Break of Rubber-Toughened Systems

Reference/preparation method	Rubber-toughened blend	Impact resistance	Strain at break (%)
This work/ <i>in situ</i> polymerization	PS60	23 ± 5 J/m	3.7 ± 0.3
	7.9A60	37 ± 1 J/m (+61%)	4.5 ± 0.4 (+22%)
	9.5A60	29 ± 1 J/m (+26%)	4.1 ± 0.1 (+11%)
	PS80	20 ± 3 J/m	3.5 ± 0.2
	8.5A80	32 ± 6 J/m (+60%)	6.3 ± 0.4 (+80%)
	10.9A80	22 ± 3 (+10%)	8.8 ± 0.4 (+150%)
38/mechanical mixing	PS	12 ± 3 J/m	3.5 ± 0.1
	PS/AES (50/50)	44 ± 5 J/m (+270%)	7.5 ± 0.7 (+114%)
23/mechanical mixing	PMMA	14 J/m	5.7
	PMMA/AES (80/20)	19 J/m (+36%)	18 (+216%)
19/ <i>in situ</i> polymerization	PS	2.9 kJ/mm <sup>2</sup>	2.5
12/ <i>in situ</i> polymerization	PS/EVA (90/10)	14.6 kJ/mm <sup>2</sup> (+403%)	15 (+500%)
	PS/SBS (93.5/6.5)	6.5 kJ/m <sup>2</sup>	
20/mechanical mixing	PS	2 kJ/m <sup>2</sup>	
	PS/EPDM (90/10)	3.0 kJ/m <sup>2</sup> (+50%)	
	PS/EPDM-g-PS (90/10)	~ 12 kJ/m <sup>2</sup> (+500%)	
	PS/EPDM (96/4)	2.5 kJ/m <sup>2</sup> (+25%)	
21/mechanical mixing	PS/EPDM-g-SMMA (96/4)	~ 10 kJ/m <sup>2</sup> (+400%)	
	PS/EPDM (94/6)	2.5 kJ/m <sup>2</sup> (+25%)	
22/mechanical mixing	PS/EPDM (94/6)	2.5 kJ/m <sup>2</sup> (+25%)	
	PS/EPDM-g-SMAH (94/6)	~ 10 kJ/m <sup>2</sup> (+400%)	

These examples from the literature for blends containing AES as the elastomer phase, for blends prepared by mechanical mixing, and for blends prepared by *in situ* polymerization and the results of this work show that the method of *in situ* polymerization used to prepare blends is potent for producing materials with comparable strains at break but lower elastomer concentrations. Other advantages of *in situ* polymerization include the good balance between the increase in the strain at break and the decrease in the Young's modulus.

### Scanning electron microscopy

Figure 8 shows micrographs of fracture surfaces resulting from the impact resistance tests for PS60, PS80, and PS/AES blends. Figure 8(a,h) shows bands of brittle fracture for PS60 and PS80, respectively, resulting from the repeated arrest and reinitiation of the fracture.<sup>38</sup> In addition, the toughened fracture surfaces [Fig. 8(b–g)] are rougher than that of PS60, and the roughness seems to be maximal for the blend containing 7.9 wt % EPDM (15.8 wt % AES) and prepared at 60°C [Fig. 8(e)]. Figure 8(i–l) shows the micrographs of the blends prepared at 80°C, and it is possible to see that the fracture surface is rougher than that of PS80. The roughness of the fracture surface indicates that PS/AES blends absorb more energy than PS during impact resistance tests. The lower roughness of the fracture surfaces is associated with lower impact resistance.

### Comparison with other rubber-toughened systems

Table III shows the impact resistance and strain at break of PS/AES blends prepared in this work and of

other rubber-toughened systems reported in the literature. The *in situ* polymerized blend prepared at 60°C containing 7.9 wt % EPDM (15.8 wt % AES) presents an impact resistance similar to the mechanically prepared PS/AES (50/50) blend, whereas the *in situ* polymerized blend polymerized at 80°C, containing 10.9 wt % EPDM (21.8 wt % AES), presents a higher strain at break. This indicates that *in situ* polymerization is a more efficient method for improving the properties of PS/AES blends with a smaller amount of AES. The enhancement of the impact resistance of about 60% for the *in situ* PS/AES blend is higher than the enhancement observed for mechanically prepared PMMA/AES (36%), also indicating the effectiveness of the *in situ* polymerization on the toughening of rigid polymers.

Table III also shows the Charpy impact resistance of two *in situ* polymerization blends, PS/EVA<sup>19</sup> and PS/SBS.<sup>12</sup> These blends present higher ratios of the impact resistance between the blends and PS than those observed for the blends prepared in this work. There are some factors that could contribute to this. One of them is the polymerization of PS in the presence of a chain transfer whose function is to promote the grafting of PS into the rubber particles. This allows the PS/EVA and PS/SBS blends to exhibit a higher toughening effect with a low rubber content. A second factor could be related to the intrinsic elastomeric properties of the different rubbers. The other factor is the mechanical characteristics of SAN, a brittle polymer that makes PS stiffer.

*In situ* polymerized PS/AES blends containing around 8 wt % EPDM present an enhancement of the impact resistance of 60% versus 50% for a PS/EPDM

blend prepared by mechanical mixing and containing 10 wt % EPDM. However, when EPDM-*g*-PS, EPDM-*g*-(styrene-*co*-methyl methacrylate) (EPDM-*g*-SMMA), and EPDM-*g*-(styrene-*co*-maleic anhydride) (EPDM-*g*-SMAH) block copolymers are used as compatibilizers, the increase in the impact resistance is very appreciable.

### CONCLUSIONS

The PS/AES blends are immiscible and present two phases: a dispersed elastomeric phase (EPDM) in a rigid matrix, whose phase behavior is strongly affected by the polymerization temperature. The blends show higher thermal stability than the PS homopolymer because of the stabilizing effect of EPDM incorporation, and the degradation of these materials is influenced by the composition and polymerization temperature. The blend prepared at 60°C with 13.0 wt % AES presented an enhancement of 60% in the impact resistance, whereas the blend prepared at 80°C with 21.8 wt % AES presented an enhancement of 150% in the strain at break. Both blends had these properties improved with a small loss in the Young's modulus. The PS/AES system shows mechanical properties similar to or better than those of the reported mechanical blends.

### References

- Galloway, J. A.; Jeon, H. K.; Bell, J. R.; Macosko, W. *Polymer* 2005, 46, 183.
- Ohishi, H.; Ikehara, T.; Nishi, T. *J Appl Polym Sci* 2001, 80, 2347.
- Katime, I.; Quintana, J. R.; Price, C. *Mater Lett* 1995, 22, 297.
- Ramsteiner, F.; Heckmann, W.; MacKee, G. E.; Breulmann, M. *Polymer* 2002, 43, 5995.
- Feng, W.; Isayev, A. I. *Polymer* 2004, 45, 1207.
- Zhang, Q.; Yang, H.; Fu, Q. *Polymer* 2004, 45, 1913.
- Cavanaugh, T. J.; Buttle, K.; Turner, J. N.; Nauman, E. B. *Polymer* 1998, 39, 4191.
- Neoh, S. B.; Hashim, A. S. *J Appl Polym Sci* 2004, 93, 1660.
- Alfarraj, A.; Nauman, E. B. *Polymer* 2004, 45, 8435.
- Saron, C.; Felisberti, M. I. *Mater Sci Eng A* 2004, 370, 293.
- Bucknall, C. B. In *Comprehensive Polymer Science*; Allen, G.; Bevington, J. C.; Eastmond, G. C.; Ledwith, A.; Russo, S.; Sigwalt, P., Eds.; Pergamon: Oxford, 1989; Vol. 10, p 27.
- Sardelis, K.; Michels, H. J.; Allen, G. *Polymer* 1987, 28, 244.
- Choi, J. H.; Ahn, K. H.; Kim, S. Y. *Polymer* 2000, 41, 5229.
- Amado, F. D. R.; Gondran, E.; Ferreira, J. Z.; Rodrigues, M. A. S.; Ferreira, C. A. *J Membr Sci* 2004, 234, 139.
- Matisová-Rychlá, L.; Rychlý, J.; George, G. A. *Polym Degrad Stab* 2002, 75, 385.
- Larocca, N. M.; Hage, E., Jr.; Pessan, L. A. *Polymer* 2004, 45, 5265.
- Tanabe, T.; Furukawa, H.; Okada, M. *Polymer* 2003, 44, 4765.
- Hwang, I. J.; Lee, M. H.; Kim, B. K. *Eur Polym J* 1998, 34, 671.
- Cheng, S.-K.; Chen, P.-T.; Wang, C.-C.; Chen, C.-Y. *J Appl Polym Sci* 2003, 88, 699.
- Shaw, S.; Singh, R. P. *J Appl Polym Sci* 1990, 40, 685.
- Shaw, S.; Singh, R. P. *J Appl Polym Sci* 1990, 40, 693.
- Shaw, S.; Singh, R. P. *J Appl Polym Sci* 1990, 40, 701.
- Turchet, R. Master's Thesis, Universidade Estadual de Campinas, 2002.
- Lu, M.; Keskkula, H.; Paul, D. R. *J Appl Polym Sci* 1995, 58, 1775.
- Lourenço, E.; Felisberti, M. I. *Polym Degrad Stab* 2006, 91, 2968.
- Sheng, J.; Li, F.-K.; Hu, J. *J Appl Polym Sci* 1998, 67, 1199.
- Keinath, S. E.; Boyer, R. F. *J Appl Polym Sci* 1981, 26, 2077.
- Hachiya, H.; Takayama, S.; Takeda, K. *J Appl Polym Sci* 1998, 70, 2515.
- Hachiya, H.; Takayama, S.; Takeda, K. *J Appl Polym Sci* 1998, 70, 2521.
- Fekete, E.; Földes, E.; Damsits, F.; Pukánszky, B. *Polym Bull* 2000, 44, 363.
- Bates, F. B.; Cohen, R. E.; Argon, A. S. *Macromolecules* 1982, 16, 1108.
- Chiantore, A.; Lazzari, M.; Ravanetti, G. P.; Nocchi, R. *J Appl Polym Sci Appl Polym Symp* 1992, 51, 249.
- Chiantore, A.; Guaita, M.; Lazzari, M. *Polymer* 1998, 39, 2777.
- Pospíšil, J.; Horak, Z.; Kruliš, Z.; Nešpůrek, S.; Kuroda, S.-I. *Polym Degrad Stab* 1999, 65, 405.
- Lourenço, E.; Felisberti, M. I. *Eur Polym J* 2006, 42, 2632.
- Bassani, A.; Hage, E., Jr.; Pessan, L. A.; Machado, A. V.; Covas, J. A. *Polim Ciênc Tecnol* 2005, 15, 176.
- Turchet, R. Ph.D. Thesis, Universidade Estadual de Campinas, 2006.
- Piorkowska, E.; Argon, A. S.; Cohen, R. E. *Polymer* 1993, 34, 4435.